

Turbulence modeling for large eddy simulation using high-order discontinuous Galerkin methods

Bachelor's thesis

Tim Dockhorn

University of Waterloo

April 2, 2018

Outline

- 1 Introduction
- 2 Large eddy simulation
- 3 Numerical discretization
- 4 The implicit large eddy simulation
- 5 Numerical results
- 6 Conclusion

Introduction

- Motions of viscous fluids are described by the Navier–Stokes equations
- Laminar flows move in parallel layers, whereas turbulent flows move chaotically (resulting in a wide range of length scales)
- Resolving all those length scales (direct numerical simulation) results in high computational costs (impractical for industry)
- Large eddy simulation resolves large-scale motions and models small-scale (universal) motions
- Use of high-order discontinuous Galerkin (DG) spatial discretization in combination with dual-splitting scheme
- Numerical dissipation is required to stabilize the scheme
- It has been found that the numerical dissipation has the ability to account for the physical dissipation of the unresolved scales

Motivation

- Does an eddy viscosity model (physical dissipation) have the ability to stabilize a discontinuous Galerkin scheme?
- Is the addition of an eddy viscosity model to the implicit large eddy simulation approach advantageous?

The filtering operation

The general filtering operation was introduced by Leonard [8] as a convolution of a unfiltered quantity $f(x, t)$ with a filter function $G(x)$

$$\bar{f}(x, t) = \int G(x - x') f(x', t) dx' \quad (1)$$

The filtered Navier–Stokes equations

The incompressible Navier–Stokes equations

$$\begin{aligned}\frac{\partial \mathbf{u}}{\partial t} + \nabla \cdot (\mathbf{u} \otimes \mathbf{u}) &= -\nabla p_k + \nabla \cdot (\nu(\nabla \mathbf{u} + (\nabla \mathbf{u})^T)) + \mathbf{f} \\ \nabla \cdot \mathbf{u} &= 0\end{aligned}\tag{2}$$

The filtered incompressible Navier–Stokes equations

$$\begin{aligned}\frac{\partial \bar{\mathbf{u}}}{\partial t} + \nabla \cdot (\overline{\mathbf{u} \otimes \mathbf{u}}) &= -\nabla \bar{p}_k + \nabla \cdot (\nu(\nabla \bar{\mathbf{u}} + (\nabla \bar{\mathbf{u}})^T)) + \bar{\mathbf{f}} \\ \nabla \cdot \bar{\mathbf{u}} &= 0\end{aligned}\tag{3}$$

The filtered Navier–Stokes equations

The set of equations differs from the Navier–Stokes equations as $\overline{\mathbf{u} \otimes \mathbf{u}} \neq \bar{\mathbf{u}} \otimes \bar{\mathbf{u}}$. The difference is called the residual-stress tensor and defined as [12]

$$\boldsymbol{\tau}^R = \overline{\mathbf{u} \otimes \mathbf{u}} - \bar{\mathbf{u}} \otimes \bar{\mathbf{u}} \quad . \quad (4)$$

The anisotropic residual-stress tensor is defined as [12]

$$\boldsymbol{\tau}^r = \boldsymbol{\tau}^R - \frac{2}{3} k_r \mathbf{I} \quad . \quad (5)$$

By plugging equation (5) into equation the filtered Navier–Stokes equations (3), we obtain an alternative form as

$$\begin{aligned} \frac{\partial \bar{\mathbf{u}}}{\partial t} + \nabla \cdot (\bar{\mathbf{u}} \otimes \bar{\mathbf{u}}) &= -\nabla \bar{p} + \nabla \cdot (\nu(\nabla \bar{\mathbf{u}} + (\nabla \bar{\mathbf{u}})^T)) + \bar{\mathbf{f}} - \nabla \cdot \boldsymbol{\tau}^r \quad , \\ \nabla \cdot \bar{\mathbf{u}} &= 0 \quad . \end{aligned} \quad (6)$$

How to model the anisotropic residual-stress tensor?

The linear eddy-viscosity assumption

$$\boldsymbol{\tau}^r \simeq -2\nu_{\text{SGS}}(\nabla \bar{\mathbf{u}} + (\nabla \bar{\mathbf{u}})^T) \quad (7)$$

The final filtered incompressible Navier–Stokes equations

$$\begin{aligned} \frac{\partial \bar{\mathbf{u}}}{\partial t} + \nabla \cdot (\bar{\mathbf{u}} \otimes \bar{\mathbf{u}}) &= -\nabla \bar{p} + \nabla \cdot ((\nu + \nu_{\text{SGS}})(\nabla \bar{\mathbf{u}} + (\nabla \bar{\mathbf{u}})^T)) + \bar{\mathbf{f}} \quad , \quad (8) \\ \nabla \cdot \bar{\mathbf{u}} &= 0 \quad . \end{aligned}$$

How to model the anisotropic residual-stress tensor?

The subgrid-scale viscosity

$$\nu_{\text{SGS}} = (C_m \Delta)^2 D_m(\bar{\mathbf{u}}) \quad , \quad (9)$$

is modeled as a function of

- a model constant C_m ,
- a characteristic filter width Δ ,
- and a differential operator D_m acting on the filtered velocity field.

Table: Desirable properties for the differential operator D_m of an eddy viscosity model [11]

P1	A positive quantity which involves only locally defined velocity gradients
P2	Cubic behavior near solid boundaries
P3	Zero for any two-dimensional flow
P4	Zero for axisymmetric or isotropic expansion/contraction

Used models

- Smagorinsky model

$$D_m = D_s = \sqrt{2\overline{S}_{ij}\overline{S}_{ij}} \quad , \quad (10)$$

where $\overline{S}_{ij} = \frac{1}{2}(\nabla_j \overline{u}_i + (\nabla_j \overline{u}_i)^T)$.

- Vreman model

$$D_m = D_v = \begin{cases} 0, & \text{if } \overline{L}_{ij}\overline{L}_{ij} = 0 \\ \sqrt{\frac{\mathcal{L}_{11}\mathcal{L}_{22}-\mathcal{L}_{12}^2+\mathcal{L}_{11}\mathcal{L}_{33}-\mathcal{L}_{13}^2+\mathcal{L}_{22}\mathcal{L}_{33}-\mathcal{L}_{23}^2}{\overline{L}_{ij}\overline{L}_{ij}}}, & \text{otherwise} \end{cases} \quad , \quad (11)$$

where $\overline{L}_{ij} = \nabla_j \overline{u}_i$ and $\mathcal{L}_{ij} = \overline{L}^T_{ik}\overline{L}_{kj}$.

Used models

- WALE model

$$D_m = D_w = \frac{(\chi_{ij}\chi_{ij})^{2/3}}{(\bar{S}_{ij}\bar{S}_{ij})^{5/2} + (\chi_{ij}\chi_{ij})^{5/4}} \quad , \quad (12)$$

where $\bar{S}_{ij} = \frac{1}{2}(\nabla_j \bar{u}_i + (\nabla_j \bar{u}_i)^T)$ and
 $\chi_{ij} = \bar{S}_{ik}\bar{S}_{kj} + \bar{\Omega}_{ik}\bar{\Omega}_{kj} - \frac{1}{3}\delta_{ij}(\bar{S}_{mn}\bar{S}_{mn} - \bar{\Omega}_{mn}\bar{\Omega}_{mn})$.

- σ -model

$$D_m = D_\sigma = \frac{\sigma_3(\sigma_1 - \sigma_2)(\sigma_2 - \sigma_3)}{\sigma_1^2} \quad , \quad (13)$$

where $\sigma_1 \geq \sigma_2 \geq \sigma_3$ are the three singular values of $\bar{L}_{ij} = \nabla_j \bar{u}_i$.

Used models

Table: Properties of the four local eddy viscosity models [11]

Model	Smagorinsky [14]	Vreman [16]	WALE [10]	σ [11]
D_m	10	11	12	13
Model constant	$C_s \approx 0.165$	$C_v \approx 0.28$	$C_w \approx 0.50$	$C_\sigma \approx 1.3$
Near-wall behavior	$\mathcal{O}(x_2^0)$	$\mathcal{O}(x_2^1)$	$\mathcal{O}(x_2^3)$	$\mathcal{O}(x_2^3)$
Vanishes for solid rotation	Yes	No	No	Yes
Vanishes for pure shear	No	Yes	Yes	Yes
Vanishes in axisymmetric case	No	No	No	Yes
Vanishes in isotropic case	No	No	Yes	Yes
Meets P1	✓	✓	✓	✓
Meets P2			✓	✓
Meets P3				✓
Meets P4				✓

Numerical discretization

- Temporal discretization is obtained by using the high-order dual splitting method introduced in [6].
- The method solves the Navier–Stokes equations in three substeps

Temporal discretization

Convective step The first step deals with the nonlinear convective term and the body force \mathbf{f} , where an explicit treatment is used for efficiency reasons. A first intermediate velocity field is obtained by evaluating the following equation

$$\frac{\gamma_0 \hat{\mathbf{u}} - \alpha_0 \mathbf{u}^n - \alpha_1 \mathbf{u}^{n-1}}{\Delta t} = -\beta_0 \nabla \cdot \mathbf{F}(\mathbf{u}^n) - \beta_1 \mathbf{F}(\mathbf{u}^{n-1}) + \mathbf{f}^{n+1}, \quad (14)$$

where a second order scheme has been used for both the BDF time integration and the extrapolation of the convective flux.

Table: Coefficients of time integration scheme and extrapolation scheme

γ_0	1	3/2
α_0	1	2
α_1	0	-1/2
β_0	1	2
β_1	0	-1

Temporal discretization

Pressure and projection step Next, the pressure at the end of the time step as well as a second intermediate (divergence-free) velocity are computed from the following formulas

$$\frac{\gamma_0 \hat{\hat{\mathbf{u}}} - \gamma_0 \hat{\mathbf{u}}}{\Delta t} = \nabla p^{n+1} \quad , \quad (15)$$

$$\nabla \cdot \hat{\hat{\mathbf{u}}} = 0 \quad . \quad (16)$$

A Poisson equation for the pressure is obtained by taking the divergence of equation (15)

$$\nabla^2 p^{n+1} = -\frac{\gamma_0}{\Delta t} \nabla \cdot \hat{\mathbf{u}} \quad . \quad (17)$$

The second intermediate velocity is then computed by using the Leray projection, i.e, projecting the intermediate velocity $\hat{\mathbf{u}}$ on divergence-free field

$$\hat{\hat{\mathbf{u}}} = \hat{\mathbf{u}} - \frac{\Delta t}{\gamma_0} \nabla p^{n+1} \quad . \quad (18)$$

Temporal discretization

Viscous step Last, the viscous term is taken into account. It is treated implicitly due to stability reasons

$$\frac{\gamma_0 \mathbf{u}^{n+1} - \gamma_0 \hat{\mathbf{u}}}{\Delta t} = \nabla \cdot ((\nu + \nu_{SGS})(\nabla \mathbf{u}^{n+1} + (\nabla \mathbf{u}^{n+1})^T)) \quad . \quad (19)$$

Temporal discretization

Boundary conditions On Γ_D we specify the value for the resolved velocity \mathbf{u} and the derivative of the pressure p [5] as

$$\mathbf{u} = \mathbf{g}_u \quad , \quad (20)$$

$$\nabla p^{n+1} \cdot \mathbf{n} = - \left[\frac{\partial \mathbf{u}^{n+1}}{\partial t} + \sum_{q=0}^{J_p-1} \beta_q ((\mathbf{u}^{n-q} \cdot \nabla) \mathbf{u}^{n-q} + \nu \nabla \times (\nabla \times \mathbf{u}^{n-q}) - \mathbf{f}^{n+1}) \right] \cdot \mathbf{n} \quad . \quad (21)$$

Note that the viscous term in the pressure boundary equation (21) is an approximation to the exact viscous term as we neglect the influence of the sub-grid scale viscosity

$$\begin{aligned} \nabla \cdot ((\nu + \nu_{SGS})(\nabla \mathbf{u} + (\nabla \mathbf{u})^T)) &= (\nu + \nu_{SGS}) \nabla^2 \mathbf{u} + (\nabla(\nu_{SGS} + \nu)) \cdot ((\nabla \mathbf{u} + (\nabla \mathbf{u})^T)) \\ &\simeq (\nu + \nu_{SGS}) \nabla^2 \mathbf{u} \simeq \nu \nabla^2 \mathbf{u} \\ &= -\nu \nabla \times (\nabla \times \mathbf{u}) \quad . \end{aligned} \quad (22)$$

Spatial discretization - Discontinuous Galerkin method

- The local Lax–Friedrichs flux is chosen in the convective step
- The symmetric interior penalty Galerkin (SIPG) method is used in the pressure step
- A modified SIPG method is used in the viscous step

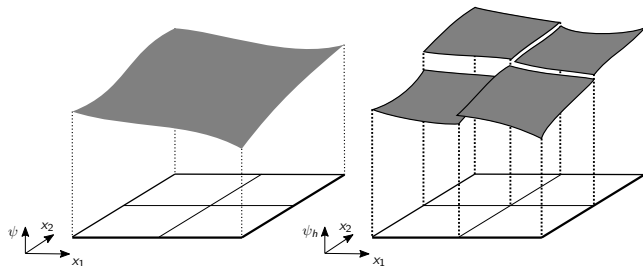


Figure: Comparison of smooth function ψ to piecewise smooth function ψ_h [1]

Instabilities and the implicit large eddy simulation

- The combination of the DG discretization with the high-order dual splitting scheme has been reported and analyzed to yield instabilities [3, 2] for small time steps.
- Krank et al. [7] demonstrated a mass-conservation error arising from the continuity equation in the under-resolved limit.
- Based on the work made in [4, 15], Krank et al. [7] introduced two penalty terms in the projection step (18) to attack these instabilities.

Instabilities and the implicit large eddy simulation

New pressure step: Find $\hat{\mathbf{u}}_h \in \mathcal{V}_h$ such that

$$\begin{aligned} & \underbrace{\left(\nabla \cdot \mathbf{v}_h, \tau_D \nabla \cdot \hat{\mathbf{u}}_h \right)_K}_{\text{div-div penalty}} + \underbrace{\left(\mathbf{v}_h, \tau_C \llbracket \hat{\mathbf{u}}_h \rrbracket \right)_{\partial K}}_{\text{jump penalty}} \\ & + \left(\mathbf{v}_h, \hat{\mathbf{u}}_h \right)_K = \left(\mathbf{v}_h, \hat{\mathbf{u}}_h \right)_K - \left(\mathbf{v}_h, \frac{\Delta t}{\gamma_0} \nabla p_h^{n+1} \right)_K \quad \forall \mathbf{v}_h \in \mathcal{V}_h, \forall K \in \mathcal{T} \quad , \end{aligned} \quad (23)$$

where the div-div and the continuity parameter are defined as $\tau_D = \Delta t \left\| \hat{\mathbf{u}}_h^{\text{mean}, K} \right\| h_{\text{eff}}$ and $\tau_C = \Delta t \left\| \hat{\mathbf{u}}_h^{\text{mean}, K} \right\|$, respectively. The effective length scale is defined as

$$h_{\text{eff}} = \frac{V_K^{1/3}}{k+1} \quad , \quad (24)$$

where V_K is the volume of the element K . The mean velocity within a given element K can be computed as

$$\left\| \hat{\mathbf{u}}_h^{\text{mean}, K} \right\| = \frac{1}{V_K} \left\| \int_K \hat{\mathbf{u}}_h d\Omega_h \right\| \quad . \quad (25)$$

Numerical results

Turbulent channel flow

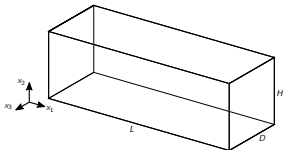


Figure: Computational domain of the turbulent channel

- The flow in a turbulent channel is one of the simplest wall-bounded turbulent flows.
- Moser et al. [9] conducted direct numerical simulations for three different friction Reynolds number.

Backward facing step

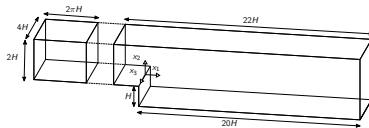


Figure: Sketch of backward facing step ($ER = 1.5$) geometry with turbulent channel as a precursor simulation

- We consider a turbulent channel flow to generate inflow data for the backward facing step.
- This method has been successfully used by Rasthofer and Gravemeier [13] (considers a backward facing step of expansion ratio $ER = 1.5$)

Turbulent channel flow

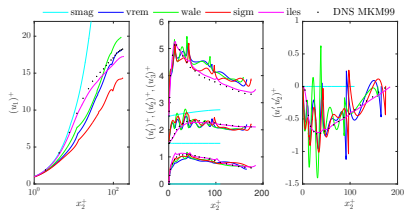


Figure: Turbulent channel flow $\text{Re}_\tau = 180$ without numerical dissipation and spatial discretization (3,3)

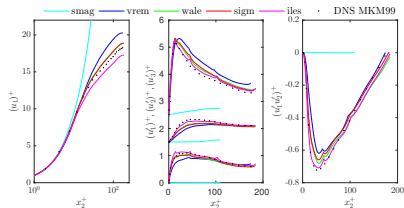


Figure: Turbulent channel flow $\text{Re}_\tau = 180$ with numerical dissipation and spatial discretization (3,3)

Turbulent channel flow

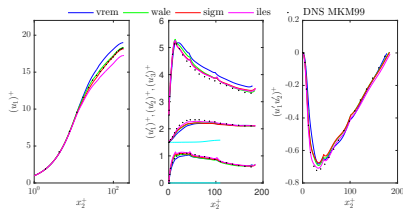


Figure: Turbulent channel flow $Re_\tau = 180$ with decreased eddy viscosity constant $C_m^{\text{new}} = C_m/\sqrt{2}$ and spatial discretization (3, 3)

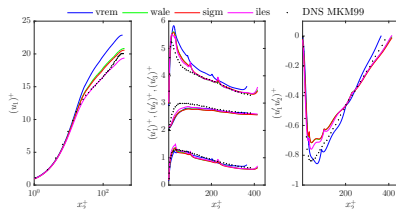


Figure: Turbulent channel flow $Re_\tau = 395$ with decreased eddy viscosity constant $C_m^{\text{new}} = C_m/\sqrt{2}$ and spatial discretization (3, 3)

Backward facing step

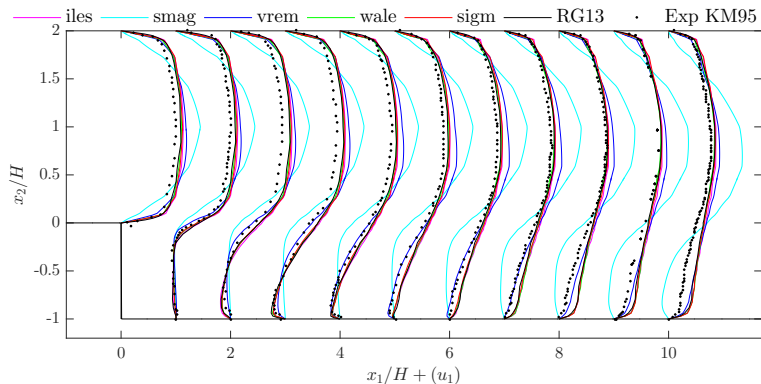


Figure: Plot of the mean velocity for combination of eddy viscosity model with numerical dissipation and spatial discretization (3, 2)

Backward facing step

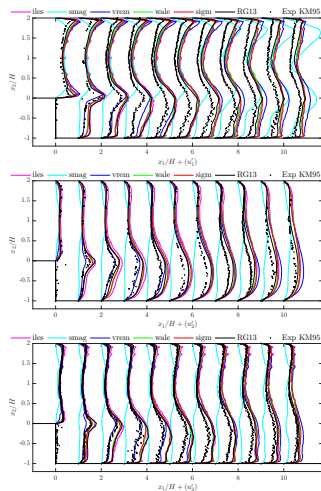


Figure: Plot of the RMS values for combination of eddy viscosity model with numerical dissipation and spatial discretization (3, 2)

Backward facing step

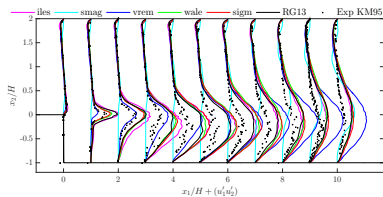


Figure: Plot of the Reynolds stress for combination of eddy viscosity model with numerical dissipation and spatial discretization (3, 2)

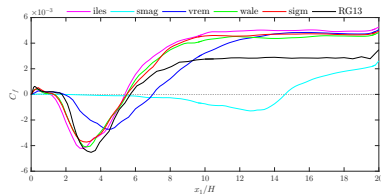


Figure: Plot of the skin friction for combination of eddy viscosity model with numerical dissipation and spatial discretization (3, 2)

Backward facing step - Computational time

The global wall time can be computed as

$$\text{Global wall time [CPUh]} = \text{computation time [s]} * \text{number of MPI processes} * \frac{1[\text{h}]}{3600[\text{s}]} \quad (26)$$

Table: Global wall time for the numerical simulations of the backward facing step
ER = 1.5

Model	iles	smag	vrem	wale	sigm
Global wall time (3, 2) in CPUh	26.532	28.364	43.253	46.493	47.161
Increase of time compared to iles in % -		6.9	63	75.2	77.8
Global wall time (2, 5) in CPUh	167.073	169.127	176.840	181.920	186.753
Increase of time compared to iles in % -		1.2	5.8	8.9	11.8

Conclusion

- Neither of the four eddy viscosity models could stabilize the DG scheme without requiring additional numerical dissipation
- The Smagorinsky turbulence model makes the originally turbulent flow laminar
- The correct cubic wall-behavior is crucial when simulating turbulence with an eddy viscosity model
- High uncertainty of obtained results with any combination of implicit large eddy simulation approach and eddy viscosity model
- The observations indicate that the product of model constant and filter width is not a constant but rather a function
$$(C_m \Delta) = f(Re, h, k)$$

- [1] N. Fehn.
A discontinuous Galerkin approach for the unsteady incompressible Navier–Stokes equations.
Master’s thesis, Insitute for Computational Mechanics, Technichal University of Munich, 2015.
- [2] E. Ferrer, D. Moxey, R. Willden, and S. Sherwin.
Stability of projection methods for incompressible flows using high order pressure-velocity pairs of same degree: continuous and discontinuous Galerkin formulations.
Communications in Computational Physics, 16(3):817–840, 2014.
- [3] E. Ferrer and R. Willden.
A high order discontinuous Galerkin finite element solver for the incompressible Navier–Stokes equations.
Computers & Fluids, 46(1):224–230, 2011.

- [4] S. M. Joshi, P. J. Diamessis, D. T. Steinmoeller, M. Stastna, and G. N. Thomsen.

A post-processing technique for stabilizing the discontinuous pressure projection operator in marginally-resolved incompressible inviscid flow.

Computers & Fluids, 139:120–129, 2016.

- [5] G. Karniadakis and S. Sherwin.

Spectral/hp element methods for computational fluid dynamics.
Oxford University Press, 2013.

- [6] G. E. Karniadakis, M. Israeli, and S. A. Orszag.

High-order splitting methods for the incompressible Navier–Stokes equations.

Journal of computational physics, 97(2):414–443, 1991.

- [7] B. Krank, N. Fehn, W. A. Wall, and M. Kronbichler.
A high-order semi-explicit discontinuous Galerkin solver for 3D incompressible flow with application to DNS and LES of turbulent channel flow.
Journal of Computational Physics, 348:634–659, 2017.
- [8] A. Leonard.
Energy cascade in large-eddy simulations of turbulent fluid flows.
Advances in geophysics, 18:237–248, 1975.
- [9] R. D. Moser, J. Kim, and N. N. Mansour.
Direct numerical simulation of turbulent channel flow up to $Re_\tau = 590$.
Physics of fluids, 11(4):943–945, 1999.
- [10] F. Nicoud and F. Ducros.
Subgrid-scale stress modelling based on the square of the velocity gradient tensor.
Flow, turbulence and Combustion, 62(3):183–200, 1999.

- [11] F. Nicoud, H. B. Toda, O. Cabrit, S. Bose, and J. Lee.
Using singular values to build a subgrid-scale model for large eddy simulations.
Physics of Fluids, 23(8):085106, 2011.
- [12] S. B. Pope.
Turbulent flows.
IOP Publishing, 2001.
- [13] U. Rasthofer and V. Gravemeier.
Multifractal subgrid-scale modeling within a variational multiscale method for large-eddy simulation of turbulent flow.
Journal of Computational Physics, 234:79–107, 2013.
- [14] J. Smagorinsky.
General circulation experiments with the primitive equations: I. the basic experiment.
Monthly weather review, 91(3):99–164, 1963.

[15] D. T. Steinmoeller, M. Stastna, and K. Lamb.

A short note on the discontinuous Galerkin discretization of the pressure projection operator in incompressible flow.

Journal of Computational Physics, 251:480–486, 2013.

[16] A. Vreman.

An eddy-viscosity subgrid-scale model for turbulent shear flow: Algebraic theory and applications.

Physics of fluids, 16(10):3670–3681, 2004.